Analysis of the Predator-Prey Model for False Whitehead (*Cnaphalocrosis medinalis*) Pests and Rice (*Oryza sativa L.*) with Holling Type II Response Function and Constant Harvesting on the Prey

Rium Hilum[1], *La Ode* Muhlis[1*], *Eka* Desti Riyan Sari[1], *Loria* Amisah Lubis[1], *Esther* Ria Matulessy[1], *Trigarcia* Maleachi Randa[1], *Chrisaria* Palungan[1], and *Dahlia Gladiola* Rurina Menufandu[1]

[1]Mathematics and Statistics Department, Faculty of Mathematics and Natural Sciences, Universitas Papua, Jalan Gunung Salju, Manokwari, 98314, Papua Barat, Indonesia

Abstract. False whitehead (Cnaphalocrosis medinalis) infestation in rice (Oryza sativa L.) is one of the main factors that cause a decline in agricultural productivity. This research aims to build and analyze a predator-prey mathematical model that describes the interaction between rice as prey and the false white grub as a predator, considering the Holling Type II response function and constant harvesting strategy on the prey. The model is constructed in the form of a system of differential equations, which are then nondimensionalized to simplify the analysis process. Next, a stability analysis was conducted on the equilibrium points with and without harvesting. The results showed that in the model without harvesting, there were two stable equilibrium points that allowed for coexistence between the two species. In the model with harvesting at certain intervals, a stable positive equilibrium point was obtained. This finding is supported by numerical simulations showing that the dynamics of the system depend on the values of the biological parameters and harvesting rate. The conclusion of this study is that controlled harvesting strategies can maintain a population balance between rice and pests and provide a theoretical basis for sustainable agricultural management based on a mathematical approach.

1. Introduction

Mathematical modeling is a method for converting intricate real-world issues into mathematical equation systems that are amenable to quantitative analyses [2]. The predator-prey model, also referred to as the Lotka-Volterra model, is a fundamental model in population dynamics. To explain the dynamic interplay between two species, predators and prey, within an ecosystem, Lotka and Volterra independently devised this model in 1925 and 1926. Predator-prey modeling is useful in agriculture when examining how pest organisms, especially insects, interact with farmed crops. Rice (Oryza sativa L.) is a vital food resource in Indonesia and other nations worldwide. Rice production management and insect control are essential components of national food security [9]. One of the pests that frequently cause serious damage to rice crops is the false whitehead, which is caused by moth attacks. This pest can attack both vegetative and generative phases, leading to a decrease in the quality and quantity of harvest [13].

A significant decrease in paddy production was reported in the Kampung Desay area of the Prafi District,

*Corresponding author: l.mukhlis@unipa.ac.id

Manokwari Regency, West Papua Province, Indonesia, which is a real-world example of this phenomenon. Based on data from [10], the harvest yield reached 5.1 tons of dry grain per hectare, but only produced about 2.5 tons of rice after milling. This decline is believed to be the result of the severity of pest attacks during different phases of plant growth. A report from [14] supports this by saying that insect infestations in the area occured from the seedling stage to just before harvest, which caused large losses in production. Harvesting tactics in a predator–prey model can be used as a mathematical solution to this problem. One approach is constant yield harvesting, in which the amount harvested per unit of time is fixed regardless of the population size [3]. This approach is crucial for achieving economic outcomes while preserving population sustainability. The response function is a crucial element in predator-prey interaction modeling, which illustrates the connection between prey population density and predation rate. Three types of response functions were identified in [5]: Type I, which is linear and typically occurs in passive predators; Type II, which exhibits an increasing but slowing relationship because of prey handling time constraints; and Type III, which is sigmoidal and represents predator adaptation to prey abundance. There is also the Holling Type IV response function, which characterizes a decline in predation efficacy in extremely high-prey populations. As noted in [15], this occurs because prey develop defense mechanisms that reduce direct interactions with predators when their populations become excessively abundant.

Several previous studies have examined the stability of predator-prey systems considering harvesting strategies. The stability and simulation of a predator-prey model with constant harvesting of the prey population were analyzed in [1]. The dynamics of an eco-epidemiological model with constant predator harvesting were investigated in [8]. Additionally, the stability of a predator–prey model with a Holling Type III response function and optimal harvesting strategies aimed at maximizing profit was studied in [6]. Based on the above description, this study aimed to analyze the stability of the predator-prey model between rice crops and false whitehead pests, considering the Holling Type II response function and the application of constant yield harvesting on the prey.

2. Research methods

This study was conducted through literature reviews and library research techniques [4, 7, 11, 12]. The following steps were followed in this study: 1. Determining the issue, putting it into quantitative terms using variables, and reviewing the literature on harvesting and predator-prey dynamics; 2. Making assumptions about the model; 3. A predator-prey model is created via compartmentalization, which builds at model based on predetermined assumptions and variables that are modified in accordance with reality; 4. Using a nondimensional model; 5. Applying linearization to the model; 6. Identifying equilibrium locations of the model; 7. Examining the equilibrium modified in points of the model for stability; and 8. Conducting numerical models.

3. Results and discussion

3.1 Problem Identification

The relationship between the false whitehead population (as a predator) and the rice population (as a prey) was identified as a problem. In the absence of predators, the population of rice will increase over time until it approaches the carrying capacity of the environment, according to current trends. The rate of population growth is disturbed if there are predators in the rice community. The false whitehead feeds on rice; hence, its

presence in the rice community undoubtedly poses a threat to the expansion of the rice population. The existence of a false whitehead in a rice community can be seen as a predator-prey relationship that can be represented mathematically and is referred to as a mathematical model.

3.2 Model presumptions

The underlying presumptions of this study are that rice and false whiteheads are thought to be closed systems, with only birth and death rates having an impact on population increase. If there is no rice population, the number of false whiteheads declines. When the community has a population of false whiteheads, the expansion of the rice population slows. In the absence of a false whitehead population in a community, the logistical growth of the rice population is constrained by its environmental carrying capacity (K). The rice population is controlled by the harvesting rate. The mortality rate of rice and false whiteheads due to external factors (the environment) were disregarded.

3.3 Constructing a mathematical model

Fig. 1 provides a clearer illustration of the compartment model of the interaction between rice as prey and a false whitehead as a predator.

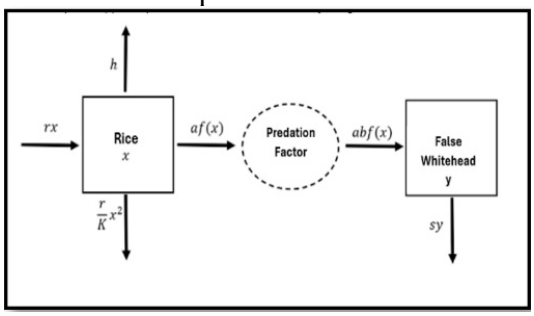

Fig1. The Compartment Model

Thus, the following system of equations is obtained, which represents the predator-prey model as follows:

$$\frac{dx}{dt} = rx\left(1 - \frac{x}{K}\right) - \frac{axy}{m+x} - h, \quad (1)$$

$$\frac{dy}{dt} = \frac{abxy}{m+x} - sy, \quad (2)$$

where *x(t)* is the prey population density at time t, *y(t)* is the predator population density at time t, *r* is the intrinsic growth rate of the prey population, *K* is the environmental carrying capacity of the prey population, h is harvesting, a is the maximum per capita predation rate, b is the energy conversion rate, m is the predation saturation level, and *s* is the predator mortality rate.

For instance, when $x = mu$, $\alpha v = \frac{ay}{rm}$, $\tau = rt$,$\beta = \frac{m}{K}$, $h = rm\bar{h}$, $y = \frac{rm\alpha v}{a}$, $\delta = \frac{ab}{r}$, and $\mu = \frac{s}{r}$ then the non-dimensional form obtained is as follows:

$$\frac{du}{d\tau} = u(1 - \beta u) - \frac{\alpha uv}{1+u} - \bar{h}, \quad (3)$$

$$\frac{dv}{d\tau} = \frac{\delta uv}{1+u} - \mu v \quad (4)$$

3.4 Linearization of the model

The general form of the Jacobian matrix of system (3, 4) is described by the following theorem.

Theorem 1. System (3, 4) has a Jacobian matrix with the general form:

$$A = \begin{bmatrix} 1 - 2\beta u - \frac{\alpha v}{(1+u)^2} & -\frac{\alpha u}{1+u} \\ \frac{\delta v}{(1+u)^2} & \frac{\delta u}{1+u} - \mu \end{bmatrix} \quad (5)$$

Proof: Suppose $du/d\tau = f_1(u, v)$ and $\frac{dv}{d\tau} = f_2(u, v)$ such that (3,4) becomes:

$$f_1(u, v) = u(1 - \beta u) - \frac{\alpha uv}{1+u} - \bar{h}, \quad (6)$$

$$f_2(u, v) = \frac{\delta uv}{1+u} - \mu v. \quad (7)$$

Then the element of the Jacobian matrix for system (3,4) can be expressed in the form:

$$A = \begin{bmatrix} \frac{\partial f_1}{\partial u} & \frac{\partial f_1}{\partial v} \\ \frac{\partial f_2}{\partial u} & \frac{\partial f_2}{\partial v} \end{bmatrix}.$$

So

$$A = \begin{bmatrix} 1 - 2\beta u - \frac{\alpha v}{(1+u)^2} & -\frac{\alpha u}{1+u} \\ \frac{\delta v}{(1+u)^2} & \frac{\delta u}{1+u} - \mu \end{bmatrix}. \quad \square$$

3.5 Finding the point of equilibrium

Assuming $du/d\tau = dv/d\tau = 0$, we can determine the equilibrium point of (3, 4) as follows:

$$u(1 - \beta u) - \frac{\alpha u v}{1+u} - \bar{h} = 0, \quad (8)$$

$$\left(\frac{\delta u}{1+u} - \mu\right) v = 0. \quad (9)$$

1) Assume that $v = 0$. Substituting this into the first equation of (3) and solving it yields $u = \frac{1 \pm \sqrt{1-4\beta\bar{h}}}{2\beta}$, where $0 \le \bar{h} \le \frac{1}{4\beta}$.

   This gives us the equilibrium points $E_{11} = \left(\frac{1-\sqrt{1-4\beta\bar{h}}}{2\beta}, 0\right)$ and $E_{12} = \left(\frac{1+\sqrt{1-4\beta\bar{h}}}{2\beta}, 0\right)$.

2) If (u^*, v^*) is a positive equilibrium point of system (3, 4), where $u^* > 0$ and $v^* > 0$ then we obtain

$$u^* = \frac{\mu}{\delta - \mu} \quad (10)$$

$$v^* = \mu\left(1 - \frac{\beta\mu}{\delta-\mu}\right)\left(\frac{\delta}{\alpha\mu(\delta-\mu)}\right) - \frac{\delta\bar{h}}{\alpha\mu}. \quad (11)$$

   where $\delta - \mu > 0$.

3.6 Analysis of Stability

Two model forms, one without harvesting and the other with a harvesting factor, were subjected to a stability analysis.

3.6.1 Analysis of Stability in the Model Without Harvesting

Model (3, 4) will change to

$$\frac{du}{d\tau} = u(1 - \beta u) - \frac{\alpha u v}{1+u} \quad (12)$$

$$\frac{dv}{d\tau} = \frac{\delta u v}{1+u} - \mu v \quad (13)$$

if we assume $\bar{h} = 0$.

The three positive equilibrium points of (12) and (13) are $E_1 = (0,0)$, $E_2 = \left(\frac{1}{\beta}, 0\right)$, dan $E_3 = \left(\frac{\mu}{\delta-\mu}, \mu\left(1 - \frac{\beta\mu}{\delta-\mu}\right)\left(\frac{\delta}{\alpha\mu(\delta-\mu)}\right)\right)$.

Theorems 2, 3, and 4 present the findings of the examination of the three equilibrium locations.

Theorem 2. The equilibrium point $E_1 = (0,0)$ is an unstable saddle point.

Proof: Since the Jacobian matrix of the equilibrium point $E_1 = (0,0)$ is $A_{E_1} = \begin{bmatrix} 1 & 0 \\ 0 & -\mu \end{bmatrix}$.
Such that $|A_{E_1} - \lambda I| = 0$ i.e.,

$$\begin{vmatrix} 1-\lambda & 0 \\ 0 & -\mu-\lambda \end{vmatrix} = 0, \quad (14)$$

Which produces the characteristic equation

$$(1-\lambda)(-\mu-\lambda) = 0, \quad (15)$$

which yields the eigenvalues λ_1 and λ_2 are

$$\lambda_1 = 1, \ \lambda_2 = -\mu. \quad (16)$$

Because λ_1, λ_2 are both real where $\lambda_1 > 0$, and $\lambda_2 < 0$, it is concluded that the equilibrium points $E_1 = (0,0)$ are unstable points. □

Theorem 3
If $(\delta - \mu) < \beta\mu$ then the equilibrium point $E_2 = \left(\frac{1}{\beta}, 0\right)$ is a stable node. ConverselyIn contrast, E_2 is an unstable node.

Proof: To prove that this theorem holds, we first need to determine the Jacobian matrix at the equilibrium point $\mathrm{E}_2 = \left(\frac{1}{\beta}, 0\right)$. By substituting each ordinate of E_2 into (5), we obtain

$$\mathrm{A}_{\mathrm{E}_2} = \begin{bmatrix} -1 & -\frac{\alpha}{\beta+1} \\ 0 & \frac{\delta}{\beta+1} - \mu \end{bmatrix} \quad (17)$$

Such that $|\mathrm{A}_{\mathrm{E}_2} - \lambda\mathrm{I}| = 0$ is

$$\begin{vmatrix} -1-\lambda & -\frac{\alpha}{\beta+1} \\ 0 & \frac{\delta}{\beta+1} - \mu - \lambda \end{vmatrix} = 0, \text{ i.e.,}$$

$$(-1-\lambda)\left(\frac{\delta}{\beta+1} - \mu - \lambda\right) = 0, \quad (18)$$

which yields the eigen values

$$\lambda_1 = -1,\ \lambda_2 = \frac{(\delta-\mu)-\beta\mu}{\beta+1}. \quad (19)$$

It appears that λ_1 and λ_2, are real. Because $\lambda_1 < 0$, only consideration is λ_2. If $(\delta-\mu) < \beta\mu$, $\lambda_2 < 0$ is obtained. This indicates that E_2 was a stable node. Conversely, if $(\delta-\mu) > \beta\mu$, then $\lambda_2 > 0$ is obtained. This condition renders E_2 an unstable node equilibrium point.□

Theorem 4

If $E_3 = \left(\frac{\mu}{\delta-\mu}, \mu\left(1-\frac{\beta\mu}{\delta-\mu}\right)\left(\frac{\delta}{\alpha\mu(\delta-\mu)}\right)\right)$ is an equilibrium point of (12, 13), then equilibrium point E_3 satisfies one of the following stability conditions:

a. E_3 is a stable node if $\mu\big((\delta-\mu)-\beta(\delta+\mu)\big)^2 \geq 4(\delta-\mu)\big((\delta-\mu)-\beta\mu\big)$ and $(\delta-\mu) < \beta(\delta+\mu)$. Otherwise, it is an unstable node if $\delta-\mu > \beta(\delta+\mu)$.
b. E_3 does not form a saddle point because for every $(\delta-\mu) > \beta\mu(\delta+\mu)$ there exists $(\delta-\mu) < \beta\mu$.
c. E_3 is a stable neutral if $\delta-\mu = \beta(\delta+\mu)$.
d. $E_3$is a stable spiral if $\mu\big((\delta-\mu)-\beta(\delta+\mu)\big)^2 > 4(\delta-\mu)\big((\delta-\mu)-\beta\mu\big)$ and $\delta-\mu < \beta(\delta+\mu)$. Conversely, it is an unstable spiral if $\delta-\mu > \beta(\delta+\mu)$. □

Proof: Let the Jacobian matrix at the equilibrium point

$$E_3 = \left(\frac{\mu}{\delta-\mu}, \mu\left(1-\frac{\beta\mu}{\delta-\mu}\right)\left(\frac{\delta}{\alpha\mu(\delta-\mu)}\right)\right),$$

be A_{E_3} and if the factorization rule is applied to (5), we obtain

$$A_{E_3} = \begin{bmatrix} a_{11} & a_{12} \\ a_{21} & 0 \end{bmatrix} \quad (20)$$

where

$$a_{11} = 1 - 2\beta u^* - \frac{\alpha v^*}{(1+u^*)^2},$$

$$a_{12} = -\frac{\alpha u^*}{1+u^*}, \qquad a_{21} = \frac{\delta v^*}{(1+u^*)^2}$$

Since $E_3 = \left(\frac{\mu}{\delta-\mu}, \mu\left(1-\frac{\beta\mu}{\delta-\mu}\right)\left(\frac{\delta}{\alpha\mu(\delta-\mu)}\right)\right)$, we obtain

$$A_{E_3} = \begin{bmatrix} \frac{\mu(\delta-\mu)-\beta\mu(\delta+\mu)}{\delta(\delta-\mu)} & -\frac{\alpha\mu}{\delta} \\ \frac{(\delta-\mu)-\beta\mu}{\alpha} & 0 \end{bmatrix} \quad (21)$$

Such that for $\left|A_{E_3} - \lambda I\right| = 0$, we obtain

$$-\lambda\left(\frac{\mu(\delta-\mu)-\beta\mu(\delta+\mu)}{\delta(\delta-\mu)} - \lambda\right) - \left(-\frac{\alpha\mu}{\delta}\right)\left(\frac{(\delta-\mu)-\beta\mu}{\alpha}\right) = 0,$$

$$\lambda^2 - \left(\frac{\mu(\delta-\mu)-\beta\mu(\delta+\mu)}{\delta(\delta-\mu)}\right)\lambda + \frac{\alpha\mu}{\delta}\left(\frac{(\delta-\mu)-\beta\mu}{\alpha}\right) = 0.$$

Where,

$$\lambda_{1,2} = \frac{\frac{\mu(\delta-\mu)-\beta\mu(\delta+\mu)}{\delta(\delta-\mu)} \pm \sqrt{\left(\frac{\mu(\delta-\mu)-\beta\mu(\delta+\mu)}{\delta(\delta-\mu)}\right)^2 - 4\frac{\mu}{\delta}\big((\delta-\mu)-\beta\mu\big)}}{2} \quad (22)$$

Thus, the following stability classification for the equilibrium point E_3 is satisfied

3.6.2 Analysis of Stability in the Model With Harvesting

The harvesting model occurs when $\bar{h} \neq 0$, i.e.,

$$\frac{du}{d\tau} = u(1-\beta u) - \frac{\alpha uv}{1+u} - \bar{h}, \quad (23)$$

$$\frac{dv}{d\tau} = \frac{\delta uv}{1+u} - \mu v. \quad (24)$$

Considering the existing model, to support the sustainability of rice and false whitehead populations, harvesting efforts must be carried out within certain control limits, that is, $0 < \bar{h} \leq \frac{1}{4\beta}$. When harvesting is performed within the interval $0 < \bar{h} < \frac{1}{4\beta}$, the equilibrium point obtained will certainly not be the same as the equilibrium point without harvesting. However, if harvesting is performed at the harvesting level $\bar{h} = \frac{1}{4\beta}$, this indicates a condition where the equilibrium point obtained is the same as the model without harvesting (this condition will not be studied further). This section focuses on harvest control within the range of $0 < \bar{h} < \frac{1}{4\beta}$, with equilibrium points at $E_{11} =$

$\left(\frac{1-\sqrt{1-4\beta\bar{h}}}{2\beta}, 0\right)$,$E_{12} = \left(\frac{1+\sqrt{1-4\beta\bar{h}}}{2\beta}, 0\right)$, and $E_3 = \left(\frac{\mu}{\delta-\mu}, \mu\left(1-\frac{\beta\mu}{\delta-\mu}\right)\left(\frac{\delta}{\alpha\mu(\delta-\mu)}\right)-\frac{\delta\bar{h}}{\alpha\mu}\right)$.

Theorem 5
If $\delta\left(1-\sqrt{1-4\beta\bar{h}}\right) < \mu\left(1+2\beta-\sqrt{1-4\beta\bar{h}}\right)$, then $E_{11} = \left(\frac{1-\sqrt{1-4\beta\bar{h}}}{2\beta}, 0\right)$ is an unstable saddle point, whereas it is an unstable node.

Proof: The Jacobian matrix at the equilibrium point $E_{11} = \left(\frac{1-\sqrt{1-4\beta\bar{h}}}{2\beta}, 0\right)$ is

$$A_{E_{11}} = \begin{bmatrix} \sqrt{1-4\beta\bar{h}} & -\frac{\alpha\left(1-\sqrt{1-4\beta\bar{h}}\right)}{1+2\beta-\sqrt{1-4\beta\bar{h}}} \\ 0 & \frac{\delta\left(1-\sqrt{1-4\beta\bar{h}}\right)}{1+2\beta-\sqrt{1-4\beta\bar{h}}}-\mu \end{bmatrix} \quad (25)$$

Such that $\left|A_{E_{11}} - \lambda I\right| = 0$ is

$$\begin{vmatrix} \sqrt{1-4\beta\bar{h}}-\lambda & -\frac{\alpha\left(1-\sqrt{1-4\beta\bar{h}}\right)}{1+2\beta-\sqrt{1-4\beta\bar{h}}} \\ 0 & \frac{\delta\left(1-\sqrt{1-4\beta\bar{h}}\right)}{1+2\beta-\sqrt{1-4\beta\bar{h}}}-\mu-\lambda \end{vmatrix} = 0 \quad (26)$$

With the characteristic equation

$$\left(\sqrt{1-4\beta\bar{h}}-\lambda\right)\left(\frac{\delta\left(1-\sqrt{1-4\beta\bar{h}}\right)}{1+2\beta-\sqrt{1-4\beta\bar{h}}}-\mu-\lambda\right) = 0 \quad (27)$$

and the eigenvalues are

$$\lambda_1 = \sqrt{1-4\beta\bar{h}},\ \lambda_2 = \frac{\delta\left(1-\sqrt{1-4\beta\bar{h}}\right)}{1+2\beta-\sqrt{1-4\beta\bar{h}}}-\mu. \quad (28)$$

Therefore, by considering the obtained eigenvalues, it can be concluded that if $\delta\left(1-\sqrt{1-4\beta\bar{h}}\right) < \mu\left(1+2\beta-\sqrt{1-4\beta\bar{h}}\right)$ the equilibrium point $E_{11} = \left(\frac{1-\sqrt{1-4\beta\bar{h}}}{2\beta}, 0\right)$ is an unstable saddle point; otherwise, it is an unstable node. □

Theorem 6
If $\delta\left(1+\sqrt{1-4\beta\bar{h}}\right) < \mu\left(1+2\beta+\sqrt{1-4\beta\bar{h}}\right)$ then the equilibrium point $E_{12} = \left(\frac{1+\sqrt{1-4\beta\bar{h}}}{2\beta}, 0\right)$ is a stable node. In constrast, E_{12} is an unstable node.

Proof: The Jacobian matrix at the equilibrium point $E_{12} = \left(\frac{1+\sqrt{1-4\beta\bar{h}}}{2\beta}, 0\right)$ is

$$A_{E_{12}} = \begin{bmatrix} -\sqrt{1-4\beta\bar{h}} & -\frac{\alpha\left(1+\sqrt{1-4\beta\bar{h}}\right)}{1+2\beta+\sqrt{1-4\beta\bar{h}}} \\ 0 & \frac{\delta\left(1-\sqrt{1-4\beta\bar{h}}\right)}{1+2\beta+\sqrt{1-4\beta\bar{h}}}-\mu \end{bmatrix} \quad (29)$$

Such that $\left|A_{E_{12}} - \lambda I\right| = 0$ i.e.,

$$\begin{vmatrix} -\sqrt{1-4\beta\bar{h}}-\lambda & -\frac{\alpha\left(1+\sqrt{1-4\beta\bar{h}}\right)}{1+2\beta+\sqrt{1-4\beta\bar{h}}} \\ 0 & \frac{\delta\left(1+\sqrt{1-4\beta\bar{h}}\right)}{1+2\beta+\sqrt{1-4\beta\bar{h}}}-\mu-\lambda \end{vmatrix} = 0 \quad (30)$$

With the characteristic equation

$$\left(-\sqrt{1-4\beta\bar{h}}-\lambda\right)\left(\frac{\delta\left(1+\sqrt{1-4\beta\bar{h}}\right)}{1+2\beta+\sqrt{1-4\beta\bar{h}}}-\mu-\lambda\right) = 0 \quad (31)$$

and the eigenvalues are

$$\lambda_1 = -\sqrt{1-4\beta\bar{h}},\ \lambda_2 = \frac{\delta\left(1+\sqrt{1-4\beta\bar{h}}\right)}{1+2\beta+\sqrt{1-4\beta\bar{h}}}-\mu \quad (32)$$

If $\delta\left(1+\sqrt{1-4\beta\bar{h}}\right) < \mu\left(1+2\beta+\sqrt{1-4\beta\bar{h}}\right)$ it can be concluded that the equilibrium point $E_{12} = \left(\frac{1+\sqrt{1-4\beta\bar{h}}}{2\beta}, 0\right)$) is a stable node; otherwise, it is an unstable node. □

Theorem 7
If $E_{13} = \left(\frac{\mu}{\delta-\mu}, \mu\left(1-\frac{\beta\mu}{\delta-\mu}\right)\left(\frac{\delta}{\alpha\mu(\delta-\mu)}\right)-\frac{\delta\bar{h}}{\alpha\mu}\right)$ is an equilibrium point of (12, 13), then the following classification satisfies the conditions for equilibrium pointE_{13}:

a. E_{13} is an unstable spiral or conversely, a stable spiral.
b. E_{13} is not a saddle point.
c. E_{13} is a stable node or, conversely, an unstable node.

Proof: Let the Jacobian matrix at equilibrium point $E_{13} = \left(\frac{\mu}{\delta-\mu}, \mu\left(1-\frac{\beta\mu}{\delta-\mu}\right)\left(\frac{\delta}{\alpha\mu(\delta-\mu)}\right)-\frac{\delta\bar{h}}{\alpha\mu}\right)$ be $A_{E_{13}}$. Using the factorization rule, we obtain

$$A_{E_{13}} = \begin{bmatrix} a_{11} & a_{12} \\ a_{21} & 0 \end{bmatrix} \quad (33)$$

where

$$a_{11} = 1-2\beta u^* - \frac{\alpha v^*}{(1+u^*)^2},$$

$$a_{12} = -\frac{\alpha u^*}{1+u^*}$$

$$a_{21} = \frac{\delta v^*}{(1+u^*)^2}, \quad a_{22} = 0$$

If $u^* = \frac{\mu}{\delta - \mu}$ and

$$v^* = \mu\left(1 \frac{\beta\mu}{\delta-\mu}\right)\left(\frac{\delta}{\alpha\mu(\delta-\mu)}\right) - \frac{\delta\bar{h}}{\alpha\mu}$$

then the Jacobian matrix at the equilibrium point $E_{13} = (u^*, v^*)$ is

$$A_{E_{13}} = \begin{bmatrix} \alpha^2\beta^2\delta\mu^3 + 2\beta\delta h - \alpha\beta\delta\mu & -\frac{\alpha\mu}{\delta} \\ \frac{\beta\mu^2\delta+\bar{h}+2\delta\bar{h}\mu-\delta^2\bar{h}}{\alpha\mu\delta} & 0 \end{bmatrix} \quad (34)$$

Such that $|A_{E_{13}} - \lambda I| = 0$ i.e.,

$$\begin{vmatrix} \alpha^2\beta^2\delta\, u^*\mu^3 + 2\beta\delta h - \alpha\beta\delta\mu - \lambda & -\frac{\alpha\mu}{\delta} \\ \frac{\beta\mu^2\delta+\bar{h}+2\delta\bar{h}\mu-\delta^2\bar{h}}{\alpha\mu\delta} & -\lambda \end{vmatrix} = 0 \quad (35)$$

$$-\lambda\,(\alpha^2\beta^2\delta\mu^3 + 2\beta\delta h - \alpha\beta\delta\mu - \lambda) - \left(-\frac{\alpha\mu}{\delta}\right)\left(\frac{\beta\mu^2\delta + \bar{h} + 2\delta\bar{h}\mu - \delta^2\bar{h}}{\alpha\mu\delta}\right) = 0,$$

$$\lambda^2 - (\alpha^2\beta^2\delta\mu^3 + 2\beta\delta h - \alpha\beta\delta\mu)\lambda + \frac{\alpha\mu}{\delta}\left(\frac{\beta\mu^2\delta + \bar{h} + 2\delta\bar{h}\mu - \delta^2\bar{h}}{\alpha\mu\delta}\right) = 0.$$

Such that

$$\lambda_{1,2} = \frac{\alpha^2\beta^2\delta\mu^3 + 2\beta\delta h - \alpha\beta\delta}{2} \pm \frac{\sqrt{(\alpha^2\beta^2\delta\mu^3 + 2\beta\delta h - \alpha\beta\delta)^2 - 4\left(\frac{\beta\mu^2\delta+\bar{h}+2\delta\bar{h}\mu-\delta^2\bar{h}}{\delta^2}\right)}}{2} \quad (36)$$

If $\alpha^2\beta^2\delta\mu^3 + 2\beta\delta h - \alpha\beta\delta\mu \geq 4\left(\frac{\beta\mu^2\delta+\bar{h}+2\delta\bar{h}\mu-\delta^2\bar{h}}{\delta^2}\right)$ and $\alpha^2\beta^2\delta\mu^3 + 2\beta\delta h < \alpha\beta\delta$ then E_{13} is unstable spiral point. □

4. Numerical simulation

Numerical simulations were conducted to confirm the orientation of trajectories in the phase plane by analyzing the system dynamics under variations in the parameters that influence the populations $u(\tau)$ and $v(\tau)$, namely α, β, δ, μ, and $\bar{h}$. Two forms of the model were considered in the simulations such that the first corresponds to a model without harvesting and the second incorporates harvesting.

4.1 Numerical simulation of the model without harvesting

In the model without harvesting, $\bar{h} = 0$, and several positive equilibrium points exist, namely E_1, E_2, and E_3. Numerical simulations were performed based on the conditions associated with each equilibrium point.

a) Simulation at Equilibrium Point E_1

For the parameter values $\delta = 0.4$, $\alpha = 1.5$, $\beta = 0.08$, and $\mu = 1.32$, the numerical simulation results shown in Fig. 2 indicate that the two eigenvalues at the equilibrium point E_1 are real and of opposite signs. This condition implies that E_1 is a saddle point and is therefore unstable. From an ecological perspective, this indicates that small perturbations in initial conditions can drive the system away from the state of total extinction. Although there are specific directions along which the system trajectories approach extinction, such behavior occurs only for a very restricted set of initial conditions. Consequently, E_1 does not serve as a stable long-term state in population dynamics.

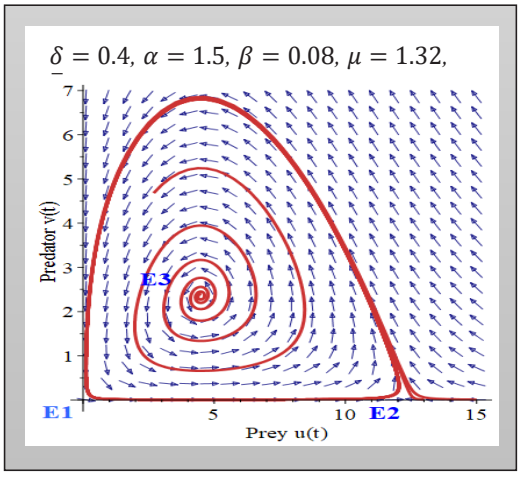

Fig 2. The point $E_1 = (0,0)$ is an unstable saddle point.

b) Simulation at Equilibrium Point E_2

When the parameters are chosen as $\delta = 0.4$, $\alpha = 2.2$, $\beta = 1.5$, and $\mu = 2{,}2$, both eigenvalues are real and negative, implying local stability, as shown in Fig.

3. In this case, the absence of predators increases the prey population toward its equilibrium level, $1/\beta$. Conversely, selecting $\delta = 2.5$, $\alpha = 1.5$, $\beta = 1.5$, and $\mu = 0.22$ yields eigenvalues with opposite signs, indicating instability in the predator-prey interaction, as shown in Fig. 4.

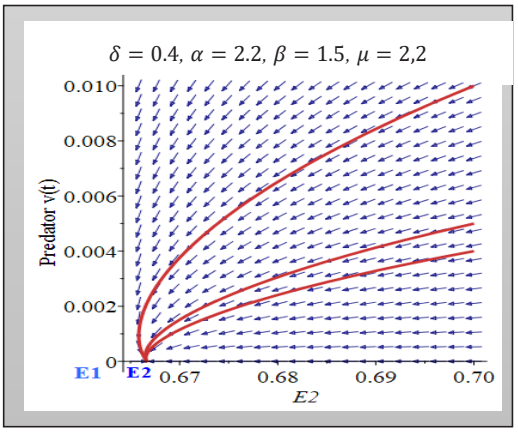

Fig 3. The point E_2 is a stable node

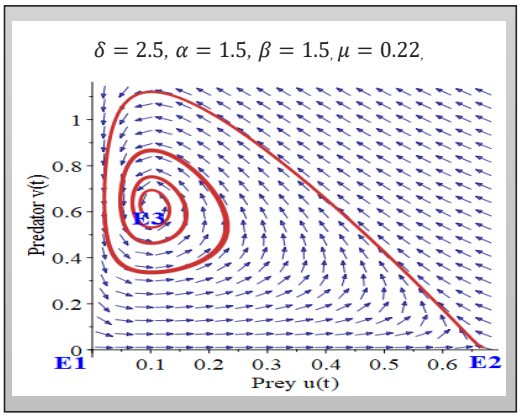

Fig 4. The point E_2 is an unstable node

c) Simulation at Equilibrium Point E_3

By considering a bounded initial population and parameter values $\delta = 2.5$, $\alpha = 5.1$, $\beta = 5.4$, and $\mu = 0.5$, two real eigenvalues are obtained, both of which are negative. This indicates that the predator–prey interaction dynamics are asymptotically stable such that the system trajectories in the phase plane converge toward the equilibrium point, as illustrated in Fig. 5. In contrast, for a different set of parameters, namely $\delta = 3.5, \alpha = 6.5, \beta = 0.3,$ and $\mu = 1.0,$ while maintaining the same initial population, the interaction dynamics underwent a qualitative change and exhibit an unstable spiral behavior. Under these conditions, both prey and predator populations oscillated with increasing amplitude, reflecting the sensitivity of population dynamics to small perturbations. Consequently, the population fluctuations tend to grow over time, and the system fails to return to the equilibrium state, as shown in Fig. 6.

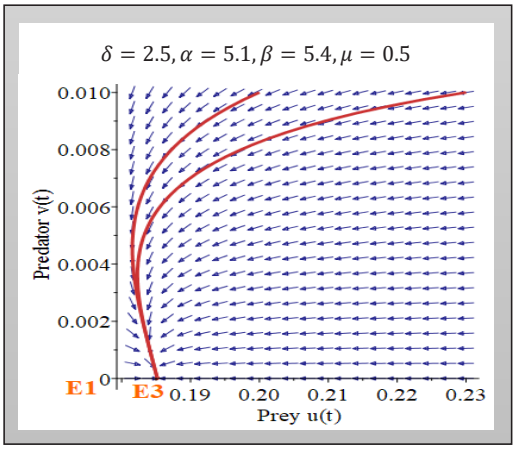

Fig 5. The point E_3 is a stable node

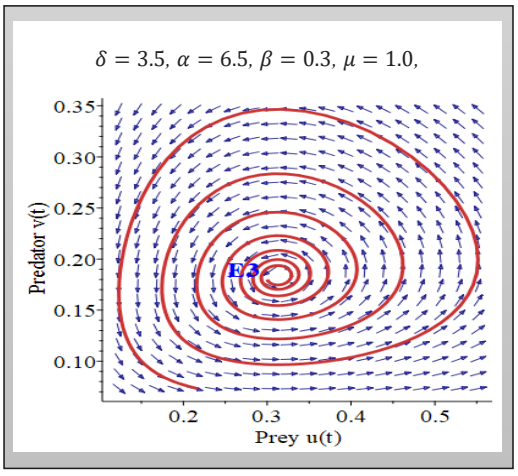

Fig 6. The point E_3 is an unstable node

4.2 Numerical Simulation of the Model Incorporating Harvesting

In this section, numerical simulations are carried out by incorporating the harvesting factor, $\bar{h}$. Under this condition, three equilibrium points are identified as the main focus of the analysis, E_{11}, E_{12}, and E_{13}. An examination of the structure

and qualitative properties of these equilibrium points indicates that E_{11} and E_{12} correspond to equilibrium point E_2 in the model without harvesting, while E_{13} corresponds to E_3. Consequently, the purpose of these numerical simulations is to explicitly investigate the impact of harvesting on the dynamic behavior of the modeled system.

a) Simulation at Equilibrium Point E_{11}

In the model without harvesting, one of the equilibrium points obtained is E_1, which exhibits stability properties in the form of a stable or unstable node. When harvesting is introduced, a corresponding equilibrium point emerges, namely E_{11}. At this equilibrium point, the system operated at a relatively low population density. This condition arises as a direct consequence of harvesting, which alters the structural dynamics of the system and induces a shift in the stability behavior toward an unstable node or a saddle point. The corresponding numerical simulation for the parameter values $\delta = 2.5$, $\alpha = 5.1$, $\beta = 5.4$, $\mu = 0.5$, $\bar{h} = \frac{1}{4}$, the corresponding numerical simulation results are presented in Fig. 7.

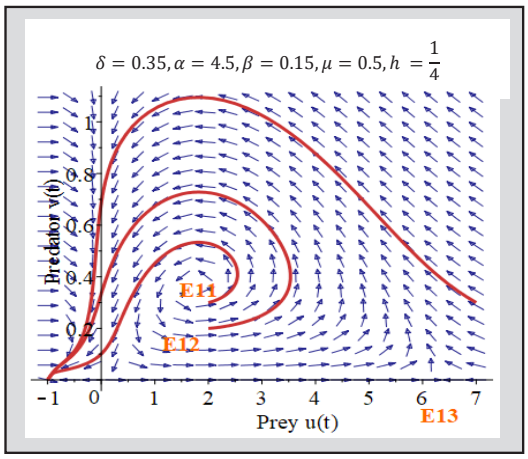

Fig. 7. The point E_{11} is an unstable saddle point.

This shift in stability behaviour affects not only the dynamics of the variable u, but also indirectly influences the dynamics of the variable v, because the predator growth rate depends functionally on the value of u through the term $\delta/(1+u)$. Consequently, the balance between predator birth and death rates became more sensitive to parameter variations. Under certain parameter configurations, the direction of the flow in the v-component may change from reinforcing to weakening, leading to modifications in the eigenvalue structure of the Jacobian matrix near the equilibrium point.

b) Simulation at Equilibrium Point E_{12}

Another equilibrium point corresponding to E_1 is E_{12}, which exhibits stability behavior identical to that of E_1 namely, a stable node or an unstable node. This equivalence in stability arises from the continuous shift in the equilibrium point induced by the harvesting effect. Although the equilibrium value of the variable u changes, the simultaneous interaction between u and v preserves the same dynamic structure, because the predator growth rate is still governed by an identical functional relationship. As long as the harvesting-induced change in u is in sufficient to alter the sign of the predator growth rate, the qualitative direction of the flow in the v-component in the neighborhood of the equilibrium point remains unchanged. At the same time, the local dynamics of the prey population around its equilibrium value undergo only smooth variations, such that the orientation of the vector field in the phase plane does not experience any structural rearrangement.

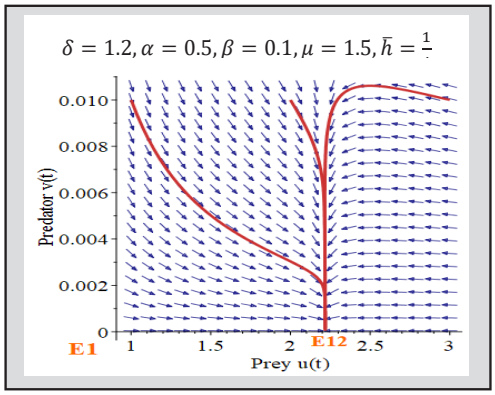

Fig 8. The point E_{12} is a stable node

Consequently, although harvesting shifts the location of the equilibrium point, the simultaneous interaction between prey and predator continues to yield the same stability configuration, namely a stable node or saddle point, as observed in the model without harvesting. Numerical simulations illustrating the behavior of the equilibrium point E_{12} are presented in Fig. 8 and 9.

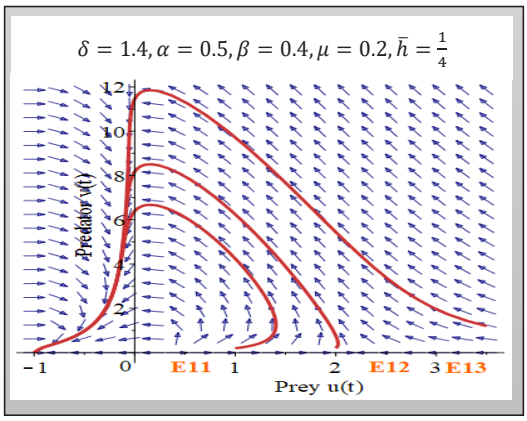

Fig 9. The point E_{12} is an unstable node

c) Simulation at Equilibrium Point E_{13}

The final simulation was conducted at equilibrium point E_{13}. As is known, E_{13} corresponds to E_3 but differs in terms of stability behavior: E_3 can exhibit neutrally stable behavior, which is absent in E_{13}. This distinction makes it particularly interesting to examine it through numerical simulations.

Focusing on the numerical simulations in the phase plane, the differences between the dynamics around E_3 and E_{13} become evident through the structure of the orbits and the evolution of the solution trajectories (u, v). In the model without harvesting $(\bar{h} = 0)$, numerical simulations around interior equilibrium E_3 showed closed orbits in the phase plane. Trajectories originating from nearby initial conditions produced oscillations in prey u and predator v with a nearly constant amplitude. Numerically, the system exhibits no tendency to converge to or diverge from the equilibrium point, resulting in cyclic and recurrent dynamics. This behavior reflects an intrinsic dynamic balance that allows neutral stability at E_3.

In contrast, for the model with harvesting $(\bar{h} \neq 0)$, the numerical simulations around the corresponding equilibrium E_{13} no longer exhibit closed orbits. All solution trajectories display a distinct tendency, either spiraling, monotonically approaching, or moving away from the equilibrium. The oscillations in u and v no longer maintain a constant amplitude; instead, they gradually dampen or amplify over time. Consequently, the numerical simulations consistently demonstrated the loss of neutral cyclic dynamics.

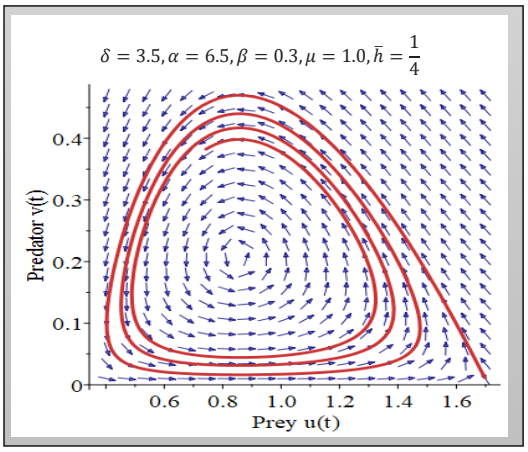

Fig 10. The point E_{13} is an unstable spiral point

The primary conclusion from these numerical simulations is that harvesting qualitatively alters the dynamic structure of the predator-prey system. Harvesting eliminates closed orbits around the interior equilibrium, thereby preventing the system from sustaining neutrally stable oscillations. Therefore, the difference between E_3 and E_{13} in numerical simulations is not merely a matter of the equilibrium location, but rather a fundamental change in the global pattern of solution trajectories, transitioning from sustained cyclic dynamics to dynamics with a clear long-term directional evolution. The simulation results for the equilibrium point E_{13}, as shown in Fig. 10.

5. Conclusion

This study examined the dynamics of interaction between rice plants (Oryza sativa L.) as prey and the false whitehead (Cnaphalocrosis medinalis) as a predator, using the Holling Type II response function and constant harvesting of the prey population. By constructing a system of differential equations and using a nondimensionalization approach, a model was obtained that represents the biological relationship between the two species, including the influence of predation rate, intrinsic growth, environmental carrying capacity, and harvesting intensity on population dynamics.

The analysis was conducted for two conditions: a model without harvesting and a model with harvesting. In the model without harvesting, several equilibrium points were obtained, including two stable points, indicating the possibility of coexistence of the rice population and pests in the ecosystem. When constant harvesting was applied, the equilibrium point and its stability characteristics changed. Within a certain harvesting interval, the system can still reach stability at a single positive equilibrium point, indicating that the populations of both species can coexist despite the exploitation efforts on the rice crop. The numerical simulations supported the analytical results and showed various patterns of system dynamics based on variations in the biological parameters and harvesting rates. This confirms that plant population management strategies for harvesting must be carried out in a controlled manner to avoid disrupting ecosystem stability.

Overall, the results of this study indicate that the predator-prey model with a Holling Type II response function and constant harvesting has the potential to be a useful tool in designing pest control strategies and sustainable agricultural management, especially in rice farming systems that are susceptible to pest attacks.

References

1. Afifah, L. I. & Pagalay, U. Analisis Kestabilan Model Prey-Predator dengan Pemanenan Konstan pada Ikan Prey. CAUCHY: Jurnal Matematika Murni dan Aplikasi 2, 194–202 (2015).
2. Aprilia, R. & Panjaitan, D. J. Pemodelan Matematika. (LPPM UMNAW, 2022).
3. Brauer, F., Castillo-Chavez, C. & Castillo-Chavez, C. Mathematical Models in Population Biology and Epidemiology. vol. 2 (Springer, 2012).
4. Chou, C.-S. & Friedman, A. Introduction to Mathematical Biology. (Springer, 2010).
5. Daud, Y., Cahyono, E., Mukhtar, N. & Sani, A. Analisis Model Matematika Mangsa-Pemangsa Holling Tipe II Dengan Faktor Pemanenan Dan Daya Dukung Lingkungan. Jurnal Matematika Komputasi dan Statistika 2, 110-114 (2022).
6. Didiharyono, D. & Irwan, M. Analisis Kestabilan dan Usaha Pemanenan Model Predator Prey Tipe Holling III dengan Keuntungan Maksimum. Jurnal VARIAN 2, 55–61 (2019).
7. Gupta, R. P. & Chandra, P. Bifurcation analysis of modified Leslie-Gower predator-prey model with Michaelis-Menten type prey harvesting. J Math Anal Appl 398, 278-295 (2013).
8. Hasan, N., Resmawan, R. & Rahmi, E. Analisis Kestabilan Model Eko-Epidemiologi dengan Pemanenan

Konstan pada Predator. Jurnal Matematika, Statistika dan Komputasi 16, 121 (2019).
9. Jamilah, J. Peluang Budidaya Tanaman Padi Sebagai Penyedia Beras Dan Pakan Ternak Menunjang Kedaulatan Pangan. (DeepPublish, 2017).
10. Mediaindonesia.com. Manokwari Diharap Jadi Lumbung Padi di Papua. Media Indonesia https://mediaindonesia.com/nusantara/559976/manokwari-diharap-jadi-lumbung-padi-di-papua (2023).
11. Mukhopadhyay, B. & Bhattacharyya, R. Effects of harvesting and predator interference in a model of two-predators competing for a single prey. Appl Math Model 40, 3264–3274 (2016).
12. Murray, J. D. Mathematical Biology: I. An Introduction. (Springer-Verlag, New York).
13. Neurafarm.com. Mengenal Hama Putih Palsu Padi dan Cara Pengendaliannya. Neurafarm https://www.neurafarm.com/blog/InfoTania/Hama&Tanaman/mengenal-hama-putih-palsu-padi-dan-cara-pengendaliannya (2022).
14. Orideknews.com. Mahasiswa PKL Polbangtan Manokwari Identifikasi Masalah Hama Padi Sawah di Kampung Aimasi. Oridek News (2020).
15. Shang, Z., Qiao, Y., Duan, L. & Miao, J. Bifurcation analysis in a predator-prey system with an increasing functional response and constant-yield prey harvesting. Math Comput Simul 190, 976–1002 (2021).